WARSAW UNIVERSITY OF TECHNOLOGY Index 351733
FACULTY OF CIVIL ENGINEERING
COMMITTEE FOR CIVIL AND WATER ENGINEERING
POLISH ACADEMY OF SCIENCES ISSN 1230-2945
DOI: 10.24425/ace.2025.153356
ARCHIVES OF CIVIL ENGINEERING
Vol. LXXI ISSUE 1 2025
pp. 655–671

Research paper

Application research of prestressed wire strand and composite mortar for flexural strengthening of T-shaped simply supported beam bridges

Xilong Zheng[1]

Abstract: In order to validate the reinforcing effect of the prestressed wire strand-composite mortar method on actual bridges, this paper applies the reinforcing method to a T-shaped simply supported beam bridge and conducts load tests before and after the reinforcement to explore its improvement effect. A finite element model was established to obtain the theoretical calculation values of the mid-span deflection and strain of the beam under test load before and after bridge reinforcement, which serve as the basis for determining the results of static load tests. Static load tests were conducted on the original bridge, and it was determined that the stiffness of the original beam was insufficient. Through a comparative analysis of data such as deflection and strain before and after reinforcement. Under partial load and medium load, the average deflection of reinforced bridge at the mid-span section of the main beam decreases by 63% and 62% respectively, indicating that the stiffness increased significantly. Compared with before strengthening, the strain of the bridge decreased by 23% and 25.5%, indicating that the strength increased significantly. The prestressed wire strand reinforcement method can significantly have a good shrinkage effect on stress cracks in bridge structures. The composite mortar can also prolong the service life of the prestressed wire strand and has good durability performance.

Keywords: prestressed wire strand and composite mortar, flexural strengthening, load test, reinforcement method

[1]PhD., Harbin University, School of Civil and Architectural Engineering, No.109 Zhongxing Da Dao, Harbin, China, e-mail: sampson88@126.com, ORCID: 0000-0001-5571-667X

1. Introduction

Highways are important national infrastructure, carrying the responsibility for social and economic development. Bridges are an essential component of highways, and the safety of bridge usage directly affects the smooth operation of the entire route [1]. With the vigorous development of the socio-economy, the demand for various goods is increasing, leading to a growing traffic volume. As a result, the traffic density and vehicle load are increasing. Meanwhile, due to the long-term exposure to natural and usage environments, a significant number of bridges are aging rapidly, experiencing severe functional decay, and can no longer meet the requirements for normal vehicle passage [2–4]. Early constructed bridges were designed with low standards, and with the passage of time, concrete material deteriorates and steel reinforcement corrodes, resulting in a reduction in the load-bearing capacity of bridges. These bridges no longer meet the requirements for transportation development [5].

Due to the high cost of bridge construction, it would require a substantial amount of funding if all the unsafe bridges were to be demolished and rebuilt. Additionally, the construction of new bridges would also take a significant amount of time [6]. If the bridges that are not suitable for modern traffic can be systematically repaired and reinforced, gradually increasing their load-bearing capacity to meet the usage standards, it would not only extend the service life of the bridges but also reduce the overall investment amount. This approach ensures that the bridges meet the required transportation capacity while avoiding the concentration of financial resources. It would bring significant economic and social benefits to the country [7–13].

Composite mortar prestressed wire strand reinforcement technology is a novel bridge structural strengthening technique. This reinforcement method utilizes small-diameter prestressed wire strands as the means of applying prestress, which is transmitted to the reinforced structure through anchors. Additionally, a composite mortar is used to bond the wire strands to the main beam, forming a unified whole [14, 15]. After reinforcement, the internal force distribution of the original structure is influenced and changed. The tensile stress on the bottom flange of the beam is reduced. Due to the application of prestressed wire strands, the main beam exhibits a certain degree of upward curvature, which unloads the beam to a certain extent and improves its flexural load-carrying capacity. It also reduces the deflection of the main beam under load and provides some shrinkage effect on the cracks that may occur under external load. The prestressed wire strands used are of high strength, low relaxation, and high ductility. The composite mortar is a new type of inorganic material with high workability, adhesion, impermeability, and non-toxicity. This reinforcement technique fully considers the excellent tensile performance of the wire strands, places the wire strands in the tension zone of the beam, and protects them with a coating of composite mortar. The excellent physical and mechanical properties of the composite mortar and the good adhesion of the interface agent are utilized. In order to verify the reinforcing effect of prestressed wire strand-composite mortar on beam bridges, the T-shaped beam bridge was reinforced and subjected to load testing before and after reinforcement.

2. Project overview

The superstructure of the bridge consists of 8×16.8 m reinforced concrete simply supported T-beams, while the substructure consists of columnar piers (abutments) and drilled pile foundations. The net bridge width is $6.5 \text{ m} + 2 \times 0.5$ m.

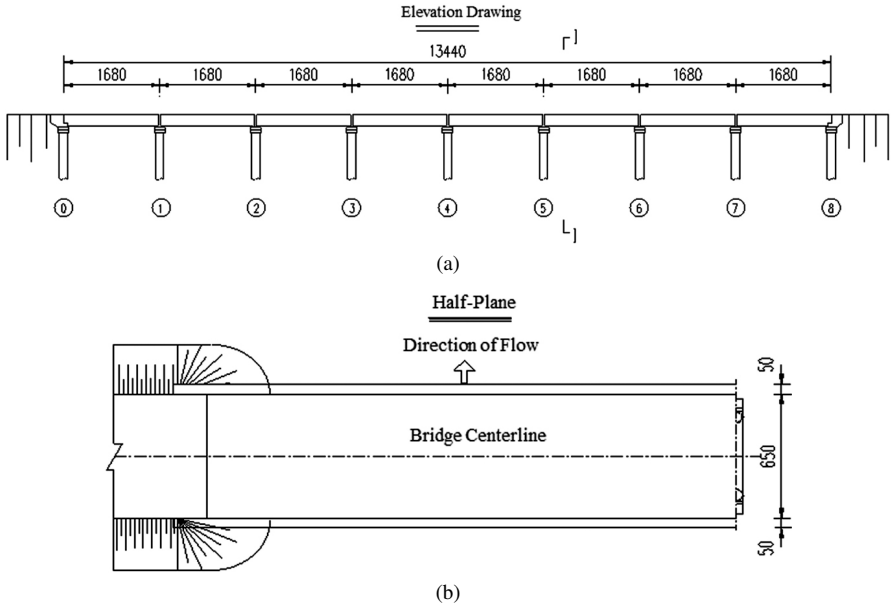

Fig. 1. Bridge layout plan (unite: cm): (a) Vertical view, (b) Plane figure

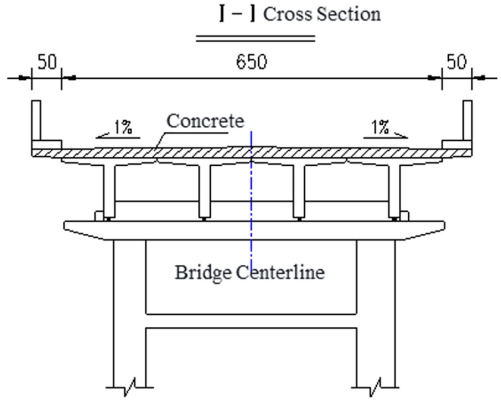

Fig. 2. Bridge cross-section drawing (unite: cm)

The bridge was built in 1967 and after years of use, the main beam has multiple concrete cracks with excessive crack widths. The bridge was originally designed to be automobile level 20. The load class of the reinforced bridge is highway grade I. The bridge is a reinforced concrete simply-supported beam bridge with a concrete grade of C40. There are vertical cracks running through the rib plates at 0.5 m intervals in the middle section of the T-beam. The reinforcement of the rib plates has severe corrosion, with some reinforcement reaching the yield strength. The transverse diaphragm has exposed reinforcement in multiple locations. The concrete pavement on the bridge deck has severe spalling, exposing the reinforcement. The bridge layout plan and cross-section drawing are shown in Fig. 1 and Fig. 2, respectively.

3. Repair and reinforcement plan

Due to the severe damage and significant deficiency in the main beam of the bridge, normal usage cannot be guaranteed, and the bridge is in an unsafe condition. To ensure the safety of vehicles crossing the bridge, effective bridge reinforcement techniques need to be implemented to address existing damages, enhance the load bearing capacity and stiffness of the main beam, and ensure the continued usability of the bridge structure, meeting the requirements of safety, suitability, and durability.

1. The main beam will be reinforced using composite mortar and prestressed steel wire ropes for cross-sectional strengthening, and using bonded steel plates for diagonal strengthening.
2. Remove the original bridge deck pavement and pour new waterproofconcrete.
3. Perform crack sealing treatment on the T-girder.
4. Repair the damaged concrete sections using epoxy resin mortar.

3.1. Prestressed steel strand arrangement and anchor design

1. Forms of prestressed steel strand arrangement
   Arrange a total of 41 prestressed steel strands separately on the bottom and sides of the T-beam. On the bottom surface of the web, arrange two layers with a total of 21 strands, while on each side surface, single-layer arrangement with 10 strands. The steel wire strand diameter is 4 mm. The ultimate strength of the steel strand is 1600 MPa, and the tensile stress is 700 MPa. After the prestressed steel strands are tensioned, apply a 3 cm thick composite mortar for surface protection. The arrangement of steel strands is shown in Figs. 3–5. The tensile stress of the bottom edge of the concrete beam section is reduced by the tension of the steel wire strand, and the constant load of the original beam is removed. The application of prestressed steel wire strand increases the bearing capacity of the main beam. The cracks in the concrete of the main beam are closed with the tension of the prestressed steel wire strand. Under the action of live load, the crack development is limited, resulting in an increase in the stiffness of the main beam.

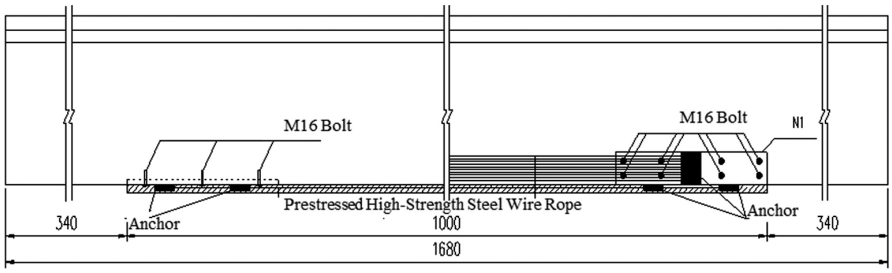

Fig. 3. Side view of the arrangement on the web (unite: cm)

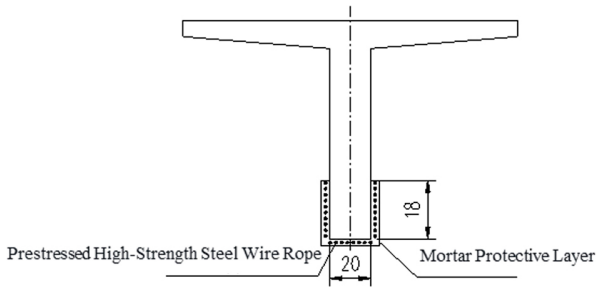

Fig. 4. Cross-sectional view of the arrangement on the web (unite: cm)

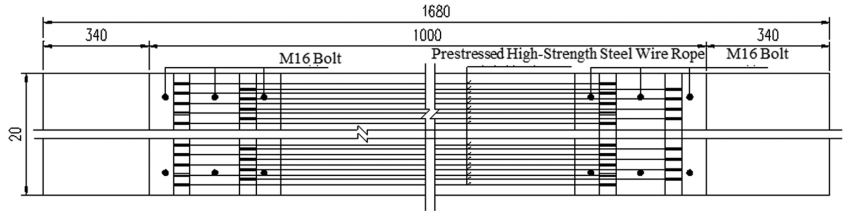

Fig. 5. Bottom view of the arrangement on the beam (unite: cm)

2. Anchor design

The anchor design is based on calculating the dimensions of the anchor based on the tensile force exerted by the steel wire rope. The net cross-sectional area after removing the prestressed steel wire rope duct should be able to withstand the tensile force of the steel wire rope. The number of layers for the arrangement of the steel wire rope is determined based on the width of the web and the quantity of prestressed steel wire ropes, which then determines the cross-sectional dimensions of the anchor. The anchor is welded to the original beam steel bar. The steel strand is tensioned by hand hoist, and symmetrical tensioning is adopted. The middle steel strand is tensioned first, and then the two sides of the steel strand are tensioned. The composite mortar is poured by spraying. For the tensioning end anchor in this strengthening design, an open-end anchor is used, while a hollow bolt anchor is used for the anchoring end anchor, as shown in Figs. 6–8.

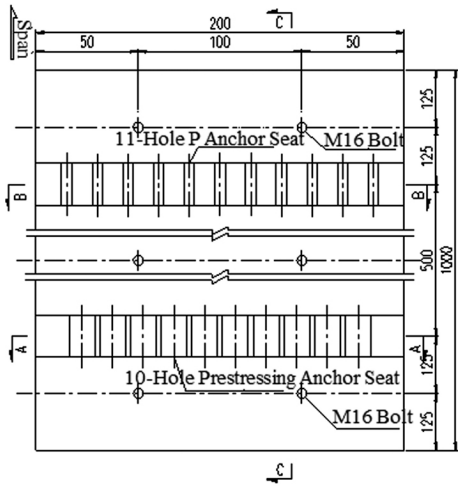

Fig. 6. Plan view of anchor 1 on the bottom of the beam (unite: cm)

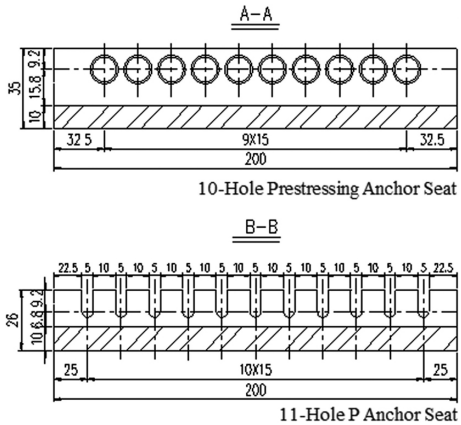

Fig. 7. Front elevation view of Anchor 1 on the bottom of the beam (unite: mm)

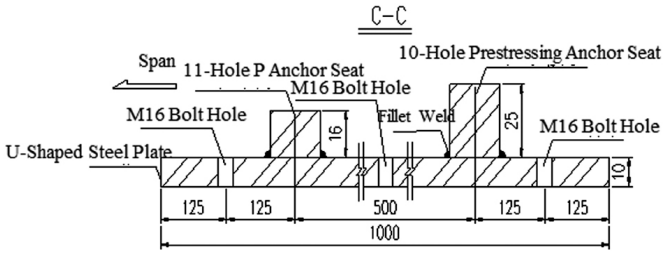

Fig. 8. Side elevation view of anchor 1 on the bottom of the beam (unite: cm)

4. Reinforcement technique

The construction process flow is shown in Figs. 9–12.

1. Surface treatment
   Remove the deteriorated concrete, such as corrosion and loosening, from the surface of the reinforced beam until a new concrete structural layer is exposed. Carry out rust removal treatment on the reinforcing bars and use epoxy resin mortar to repair and level the surface. Seal the cracks.
2. Chiseling of beam end notches
   Based on the design, determine the positions for installing anchors at both ends of the beam, and chisel the notches with a depth of 15 mm. Apply adhesive to anchor steel plates along the width direction, and secure the anchor plates by embedding bolts and gluing the steel plates.
3. Production and fixation of anchors
   Produce anchors according to the design requirements and the number of steel wires, and weld them onto the anchor-attached steel plates.

Fig. 9. End groove

Fig. 10. End anchor

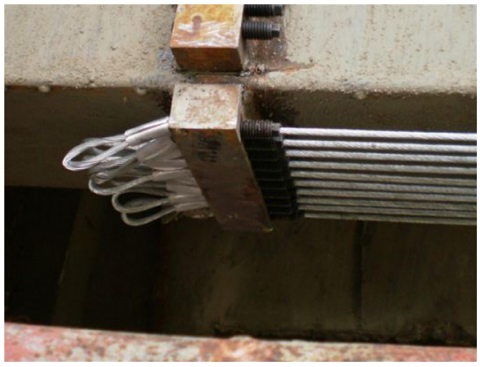

Fig. 11. Wire rope anchorage

Fig. 12. Reinforced Beam

4. Setting of reaction points
   In order for the post-tensioned steel wire rope to exert an upward equivalent load on the beam, and considering that the steel wire rope cannot have fully compact contact with the bottom of the beam due to construction reasons, fine round steel bars with a diameter of 10 mm are embedded in the bottom of the beam as reaction points.
5. Steel wire rope cutting and extrusion anchor head fabrication
   The cutting length is determined based on the spacing between the two end anchors and the working stress of the prestressed steel wire rope. It is necessary to ensure that the steel wire rope is in a tensioned state during the cutting process. After cutting, use specially designed extrusion anchor heads to extrude aluminum alloy sleeves to tightly combine them with the steel wire rope.
6. Steel wire rope tensioning and anchoring
   On one side, the end of the steel wire rope can be directly inserted into the anchor, while the other end is tensioned by a specialized tensioning device. After tensioning, the elongated aluminum sleeve is anchored when it exceeds the anchor. Following the principle of symmetry, the tensioning is gradually carried out symmetrically from both sides towards the center. The difference in the number of steel wire ropes on both sides should not exceed 3 to prevent structural torsion or lateral bending.
7. Protective coating with composite mortar
   The composite mortar should be applied in layers. The edge formwork should be positioned according to the design thickness, and the working surface should be leveled. Apply the mortar in layers, and the time interval between each application is determined when the previous layer is no longer sticky to the touch. The second layer should be applied when the mortar from the previous layer is no longer sticky to the touch.

5. Comparison and analysis of static load test results before and after reinforcement

Due to the significant number of cracks and severe damage observed in the third span of this bridge, which represents a typical case, static load tests were conducted before and after reinforcement on the bridge's third span. The reinforcement effectiveness was analyzed through the deflection of the main beam (to assess changes in structural stiffness) and the strain on the main beam (to evaluate changes in structural strength). Based on on-site measurement data, a finite element beam grid model of the bridge was constructed using MIDAS/CIVIL software. The theoretical displacements and strains of the bridge under the test loads were calculated using this model, serving as the basis for the experimental loading. The finite element model of the bridge is built using the beam lattice method. The main beam and the transverse beam are simulated by beam element. One side of the main beam is a fixed support, and the other side is a movable support. The finite element model is shown in Fig. 13.

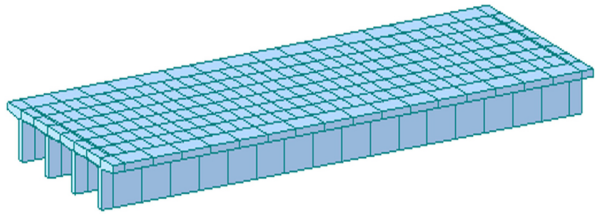

Fig. 13. Finite element model of T-beam

5.1. Test plan

1. Strain point layout
   Strain points N1~N7 are arranged on the side of the cross-section of the T-beam in the mid-span. Deflection points M1~M4 are arranged on the bottom surface of the cross-section of the beam. The layout of the measurement points is shown in Fig. 14.

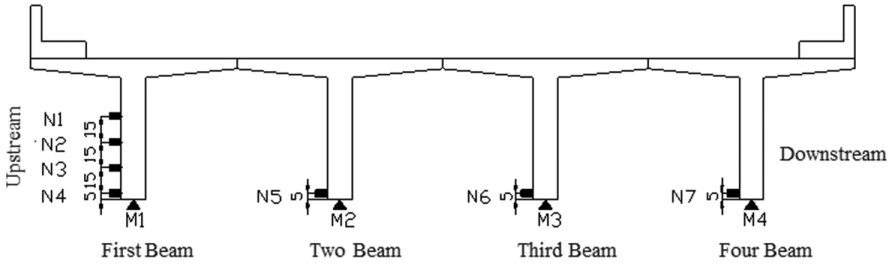

Fig. 14. Layout of measurement points on the cross-section at mid-span of the test span

2. Test load and layout
   In order to simulate the maximum bending moment effect and ensure the effectiveness of the test, two heavy vehicles with a weight of 330 kN each were used as the test load. A load efficiency of 97% was employed to simulate the Highway Class II load, ensuring the efficiency of the test load. The detailed axle loads of the vehicles are shown in Table 1.

Table 1. Summary of loaded vehicle axle weights (kN)

Serial Number	Front Axle Load	Middle Axle Load	Rear Axle Load	Gross Weight
1	66	132	132	330
2	66	132	132	330

Taking into account the specific conditions of the bridge and the layout method for the most unfavorable operating conditions, the test load for this experiment is arranged in two categories: offset load and centered load. The vehicle loading layouts are shown in Fig. 15–18.

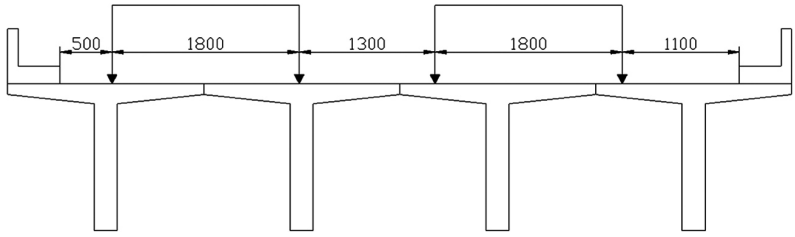

Fig. 15. Diagram of transverse offset load vehicle arrangement (unite: mm)

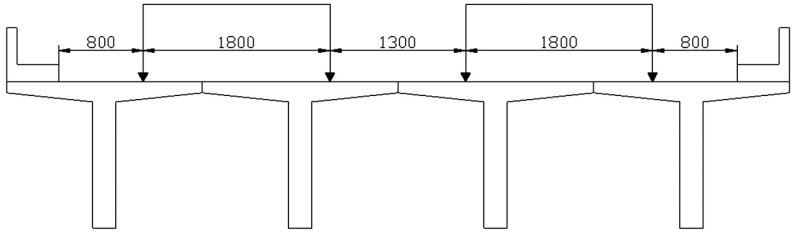

Fig. 16. Diagram of transverse centered load vehicle arrangement (unite: mm)

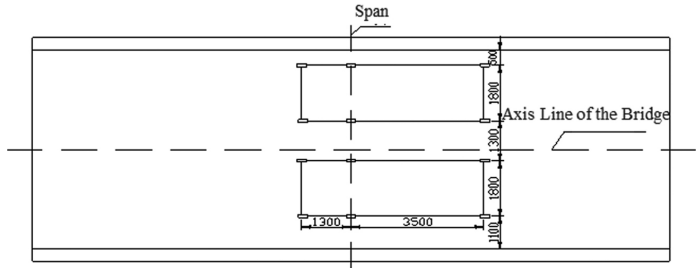

Fig. 17. Diagram of offset load vehicle plan layout (unite: mm)

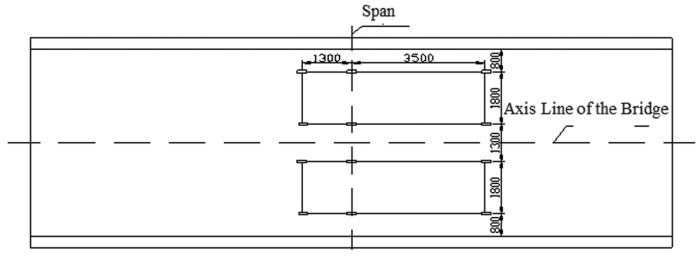

Fig. 18. Vehicle interior layout diagram (unite: mm)

5.2. Deflection analysis

Mainly by measuring the deflection values at the mid-section of the main beams in the third span, the stiffness of the main beams is tested.

Under the condition of asymmetric loading, the theoretical calculation values of deflection generated by each main beam before reinforcement are shown in Fig. 19, and the comparison between the theoretical values and the measured values of the deflection at the mid-section is shown in Table 2.

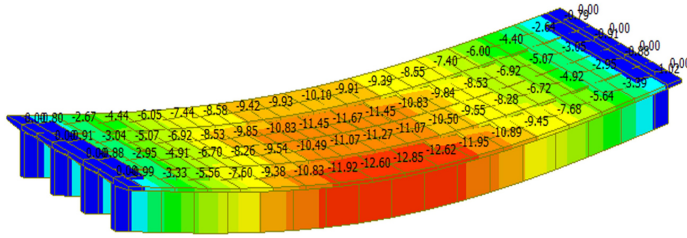

Fig. 19. Theoretical value of deflection of the main beam under pre-strengthening asymmetric loading condition

Table 2. Comparison of measured and theoretical values of deflection at midspan sections of main beams (mm)

Measurement point	M1	M2	M3	M4
Theoretical value	8.40	8.05	8.15	7.79
Actual value	4.60	3.85	4.33	3.49
Residual strain	0.37	0.23	0.43	0.25
Relative residual displacement	0.08	0.06	0.10	0.07
Verification coefficient	0.55	0.48	0.53	0.45

Under moderate loading condition, the theoretical calculation values of deflection for each reinforced main beam are shown in Fig. 20. The comparison between theoretical and measured values of deflection at midspan sections is presented in Table 3. The deflection verification coefficient is the ratio of the measured value to the theoretical value.

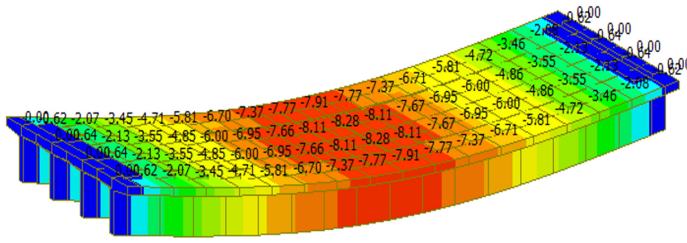

Fig. 20. Theoretical values of deflection for reinforced main beams under moderate loading condition

Table 3. Comparison of measured and theoretical values of deflection at midspan sections for each main beam

Measurement point	M1	M2	M3	M4
Theoretical value (mm)	7.91	8.28	8.28	7.91
Actual value (mm)	4.06	4.32	4.56	3.82
Verification coefficient	0.51	0.52	0.55	0.48

Based on Table 3, it can be concluded that:

Under the action of vehicle loads, the verification coefficient of deflection at midspan sections is between 0.45 and 0.55, which meets the requirement in the "Technical Specifications for Testing and Evaluation of Bridge Load-bearing Capacity" (JTG/T J21-2011) that the verification coefficient should be less than 1. This indicates that each main beam has sufficient safety margin. The relative residual displacements at various measuring points on the main beams are all less than 20%, indicating that the main beams of the bridge have good elastic recovery ability after unloading.

Based on Fig. 21 and Fig. 22, it can be concluded that the measured deflection curve of the bridge follows a similar trend to the theoretically calculated deflection curve, indicating reliable test data. Under partial load and medium load, the average deflection at the mid-span section of the main beam decreases by 63% and 62% respectively. After reinforcement with prestressed steel wire ropes, the overall stiffness of the bridge significantly improves compared to before reinforcement.

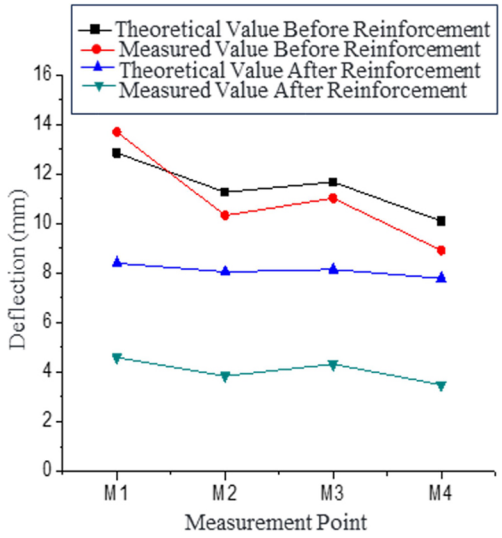

Fig. 21. Comparison chart of deflection of main beams before and after reinforcement under partial load

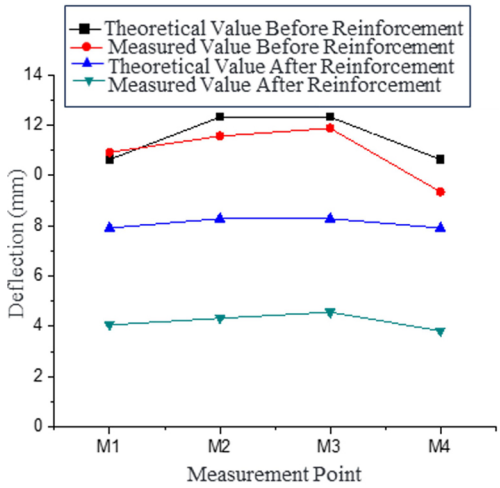

Fig. 22. Comparison of deflection in the main beam before and after reinforcement under load

5.3. Stress (strain) analysis

By primarily testing the strain values at the mid-span sections of the main beams of the third span, the strength condition of the main beams is assessed. The measured strain values at various locations of the control sections during the load test are incremental values after loading, with tensile stress denoted as positive. The following analysis compares the measured incremental strain values with the theoretically calculated values. The comparison between the measured and theoretically calculated strain values at the mid-span before reinforcement is presented in Table 4 and Table 5. The strain variation coefficient is the ratio of the measured value to the theoretical value.

Table 4. Comparison of measured and theoretical values of mid-span strain under unbalanced load conditions

Measurement point	**N1**	**N2**	**N3**	**N4**	**N5**	**N6**	**N7**
Theoretical value ($\mu\varepsilon$)	81	173	265	356	255	325	223
Actual value ($\mu\varepsilon$)	94	197	290	565	295	505	285
Verification coefficient	1.16	1.14	1.09	1.59	1.16	1.55	1.28

Table 5. Comparison of measured and theoretical values of mid-span strain under medium load conditions

Measurement point	**N1**	**N2**	**N3**	**N4**	**N5**	**N6**	**N7**
Theoretical value ($\mu\varepsilon$)	45	109	173	237	344	344	237
Actual value ($\mu\varepsilon$)	56	126	191	386	466	534	316
Verification coefficient	1.24	1.16	1.10	1.63	1.35	1.55	1.33

Under the action of test loads, the main beam of the bridge has experienced concrete cracking, with a relatively large measured strain value at the mid-span section. The maximum measured value is 565 $\mu\varepsilon$. The concrete strain verification coefficients range from 1.09 to 1.63, indicating that the strength of the main beam does not meet the design requirements. Some sections of the main beam have a relative residual strain exceeding 20%, indicating that these sections do not have good elastic recovery capability after unloading.

The application of prestressed steel strands at the bottom of the beam increases the reinforcement ratio of the beam section and introduces a negative bending moment into the structure, resulting in compressive stress at the bottom of the main beam. Under the condition of skewed loads, the stress distribution of the reinforced main beam is shown in Fig. 23, and the comparison between the theoretical and measured values of strain at each mid-span section of the main beam is shown in Table 6. The strain variation coefficient is the ratio of the measured value to the theoretical value.

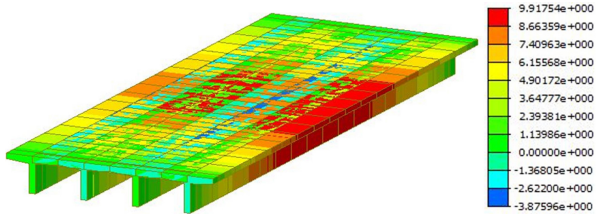

Fig. 23. Stress distribution of the main beam under skewed load condition (MPa)

Table 6. Comparison of measured and theoretical values of mid-span strain under skewed load condition

Measurement point	**N1**	**N2**	**N3**	**N4**	**N5**	**N6**	**N7**
Theoretical value ($\mu\varepsilon$)	64	130	197	264	213	248	202
Actual value ($\mu\varepsilon$)	12	52	90	130	85	99	76
Verification coefficient	0.19	0.40	0.46	0.49	0.40	0.40	0.38

Under medium load condition, the stress distribution of the reinforced main beam is shown in Fig. 24. The comparison between the theoretical calculated values and the measured values of strain at each mid-span section of the main beam is presented in Table 7. The strain variation coefficient is the ratio of the measured value to the theoretical value.

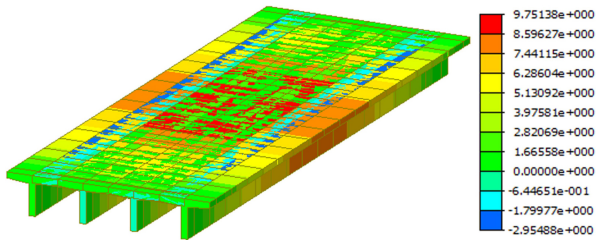

Fig. 24. Stress distribution of the main beam under medium load condition (MPa)

Table 7. Comparison between measured and theoretical values of mid-span strain under medium load condition

Measurement point	**N1**	**N2**	**N3**	**N4**	**N5**	**N6**	**N7**
Theoretical value ($\mu\varepsilon$)	53	105	158	211	261	261	211
Actual value ($\mu\varepsilon$)	9	40	72	106	128	136	100
Verification coefficient	0.17	0.38	0.46	0.50	0.49	0.52	0.47

Based on Table 7, the maximum measured strain at the mid-span section of the strengthened main beam under eccentric load condition is 130 $\mu\varepsilon$, and under medium load condition is 136 $\mu\varepsilon$. These values represent a reduction of 23% and 25.5% respectively compared to before strengthening. The significant decrease in strain indicates an improvement in the strength of the structure after reinforcement. The concrete strain coefficient ranges from 0.17 to 0.52, all of which satisfy the specification requirements. During the test, there were no noticeable residual deformations observed after unloading, indicating that the strengthened structure remains in an elastic state.

According to Fig. 25 and Fig. 26, it can be observed that the calculated and measured values of strain after reinforcement show a significant decrease compared to before reinforcement. This indicates that the reinforcement technique can effectively improve the strength of the main beam structure. The measured strain curve closely follows the trend of the calculated strain curve, indicating that the actual loading conditions of the main beam are relatively consistent with the theoretical calculations. Additionally, the post-reinforcement concrete strain values along the height of the beam are mostly aligned in a straight line, indicating that the reinforced beam exhibits good overall working performance in terms of strain conformity with the assumption of a plane section.

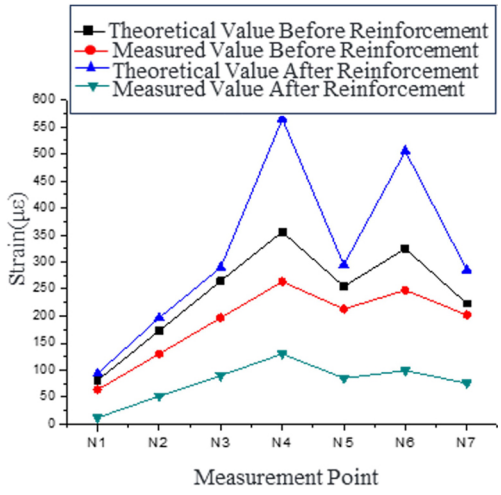

Fig. 25. Comparison of strain on the main beam before and after reinforcement under eccentric load condition

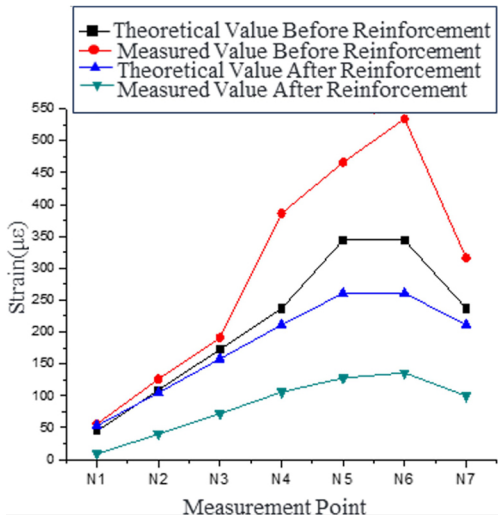

Fig. 26. Comparison of strain on the main beam before and after reinforcement under eccentric load condition

6. Conclusions

Through the reinforcement design of a simply supported T-shaped reinforced concrete beam bridge, the application of prestressed steel strand-composite mortar reinforcement technology in bridge reinforcement is introduced. The conclusions are as follows:

1. The bending bearing capacity of the original bridge was calculated and it was determined that the original beam's load-bearing capacity could not meet the Highway Class II load. The reinforcement design scheme for the concrete T-shaped beam bridge is proposed, which involves reinforcing the side and bottom surfaces of the T-beam rib with prestressed steel strands and then covering them with composite mortar.
2. A finite element model was established to obtain the theoretical calculation values of the mid-span deflection and strain of the beam under test load before and after bridge reinforcement, which serve as the basis for determining the results of static load tests. Static load tests were conducted on the original bridge, and it was determined that the stiffness of the original beam was insufficient. Under partial load and medium load, the average deflection of reinforced bridge at the mid-span section of the main beam decreases by 63% and 62% respectively, indicating that the stiffness increased significantly.
3. The bearing capacity of the reinforced bridge was tested, and a comparison was made between the theoretical values and the measured values, thereby verifying that the composite mortar prestressed steel strand reinforcement technology can achieve the expected reinforcement effect. Compared with before strengthening, the strain of the bridge decreased by 23% and 25.5%, indicating that the strength increased significantly.

References

[1] P. Hou, J. Yang, Y. Pan, et al., "Experimental and simulation studies on the mechanical performance of concrete T-Girder bridge strengthened with K-Brace composite trusses", *Structures*, vol. 43, pp. 479–492, 2022, doi: 10.1016/j.istruc.2022.06.069.

[2] A.M. Okeil, S. El-Tawil, and M. Shahawy, "Flexural reliability of reinforced concrete bridge girders strengthened with carbon fiber-reinforced polymer laminates", *Journal of Bridge Engineering*, vol. 7, no. 5, pp. 290–299, 2002, doi: 10.1061/(ASCE)1084-0702(2002)7:5(290).

[3] D. Schnerch, M. Dawood, S. Rizkalla, and E. Sumner, "Proposed design guidelines for strengthening of steel bridges with FRP materials", *Construction and Building Materials*, vol. 21, no. 5, pp. 1001–1010, 2007, doi: 10.1016/j.conbuildmat.2006.03.003.

[4] J. Yang, P. Hou, Y. Pan, et al., "Shear behaviors of hollow slab beam bridges strengthened with high-performance self-consolidating cementitious composites", *Engineering Structures*, vol. 242, art. no. 112613, 2021, doi: 10.1016/j.engstruct.2021.112613.

[5] C. Czaderski and M. Motavalli, "40-Year-old full-scale concrete bridge girder strengthened with prestressed CFRP plates anchored using gradient method", *Composites Part B: Engineering*, vol. 38, no. 7-8, pp. 878–886, 2007, doi: 10.1016/j.compositesb.2006.11.003.

[6] A.H. Al-Saidy, F.W. Klaiber, T.J. Wipf, et al., "Parametric study on the behavior of short span composite bridge girders strengthened with carbon fiber reinforced polymer plates", *Construction and Building Materials*, vol. 22, no. 5, pp. 729–737, 2008, doi: 10.1016/j.conbuildmat.2007.01.020.

[7] M. Herbrand, V. Adam, and M. Classen, "Strengthening of existing bridge structures for shear and bending with carbon textile-reinforced mortar", *Materials*, vol. 10, no. 9, pp. 1099, 2017, doi: 10.3390/ma10091099

[8] M. Al-Emrani, and R. Kliger, "Analysis of interfacial shear stresses in beams strengthened with bonded prestressed laminates", *Composites Part B: Engineering*, vol. 37, no. 4-5, pp. 265–272, 2006, doi: 10.1016/j.compositesb.2006.01.004.

[9] B. Pang, P. Yang, Y. Wang, et al., "Life cycle environmental impact assessment of a bridge with different strengthening schemes", *The International Journal of Life Cycle Assessment*, vol. 20, pp. 1300–1311, 2015, doi: 10.1007/s11367-015-0936-1.

[10] J. Yang, R. Chen, Z. Zhang, et al., "Experimental study on the ultimate bearing capacity of damaged RC arches strengthened with ultra-high performance concrete", *Engineering Structures*, vol. 279, pp. 115611, 2023, doi: 10.1016/j.engstruct.2023.115611.

[11] W. Hu, Y. Li, and H. Yuan, "Review of experimental studies on application of FRP for strengthening of bridge structures", *Advances in Materials Science and Engineering*, vol. 2020, pp. 1–21, 2020, doi: 10.1155/2020/8682163.

[12] E. Beneberu and N. Yazdani, "Residual strength of CFRP strengthened prestressed concrete bridge girders after hydrocarbon fire exposure", *Engineering Structures*, vol. 184, pp. 1–14, 2019, doi: 10.1016/j.engstruct.2019.01.057.

[13] A. Hosseini, E. Ghafoori, R. Al-Mahaidi, et al., "Strengthening of a 19th-century roadway metallic bridge using nonprestressed bonded and prestressed unbonded CFRP plates", *Construction and Building Materials*, vol. 209, pp. 240–259, 2019, doi: 10.1016/j.conbuildmat.2019.03.095.

[14] X. Li, G. Wu, M. S. Popal, et al., "Experimental and numerical study of hollow core slabs strengthened with mounted steel bars and prestressed steel wire ropes", *Construction and Building Materials*, vol. 188, pp. 456–469, 2018, doi: 10.1016/j.conbuildmat.2018.08.073.

[15] Z.Q. Liu, Z.X. Guo, and Y. Ye, "Flexural behavior of RC beams strengthened with prestressed steel wire ropes polymer mortar composite", *Journal of Asian Architecture and Building Engineering*, vol. 21, no. 1, pp. 48–65, 2022, doi: 10.1080/13467581.2021.1928508.

Received: 2023-12-23, Revised: 2024-03-19